NCAR CESM2 release of CAM-SE: A reformulation of the spectral-element dynamical core in dry-mass vertical coordinates with comprehensive treatment of condensates and energy

P. H. Lauritzen[1]*, R.D. Nair[1], A.R. Herrington[2], Steve Goldhaber[1], Julio T. Bacmeister[1], B. Eaton[1], C.M. Zarzycki[1], A. Gettelman[1], P. Callaghan[1], R.B. Neale[1], Mark A. Taylor[3], K.A. Reed[2]

[1]National Center for Atmospheric Research
[2]School of Marine and Atmospheric Sciences, Stony Brook University, State University of New York, Stony Brook, New York
[3]Sandia National Laboratories, Albuquerque, New Mexico

Key Points:

- = enter point 1 here =
- = enter point 2 here =
- = enter point 3 here =

*1850 Table Mesa Drive, Boulder, Colodaro, USA

Corresponding author: peter Hjort Lauritzen, pel@ucar.edu

Abstract
It is the purpose of this paper to document the new NCAR version of the spectral-element (SE) dynamical core as part of the CESM2.0 release. This version differs from previous releases of the SE dynamical core in several ways. Most notably the hybrid-sigma vertical coordinate is based on dry pressure, the condensates are dynamically active in the thermodynamic and momentum equations (also referred to as condensate loading), and the continuous equations of motion conserve a more comprehensive total energy that includes condensates. The code base has been significantly reduced as part of integrating SE as a dynamical core in the CAM (Community Atmosphere Model) repository rather than importing the SE dynamical core from HOMME (high-order method modeling environment) as an external.

1 Introduction

The high-order method modeling environment (HOMME) is framework for developing new generation computationally efficient and petascale capable dynamical cores for the community atmospheric model (CAM). HOMME employs high-order method such as the spectral element (SE) and discontinuous Galerkin methods on a cubed-sphere, for solving equations of motion and it can be configured to solve hydrostatic primitive equations *Thomas and Loft* [2000]; *Taylor et al.* [2008]; *Nair et al.* [2009]. A version of SE dynamical core in HOMME has been integrated into the CAM frame work known as the CAM-SE *Dennis et al.* [2012] and released with CAM5 [*Neale et al.*, 2010] ... DEFINE CESM1.5 SE

IS $\Delta p_k m_k^{(d)}$ tracer mass? or pseudo-mass????

- formulation with the least changes to the existing CAM-SE modeling system
- why convert: physics dynamics coupling, conversion can violate shape-preservation, ...

2 Continuous equations

Before writing the continuous equations of motion using a dry-mass vertical coordinate, we first need to discuss the representation of water variables (section 2.1), discuss the ideal gas law and derive the thermodynamic equation for a mixture containing all water variables not just water vapor (section 2.2). The discussion of the equations of motion in the presence of water vapor, cloud liquid and ice closely follows *Staniforth et al.* [2006]. Thereafter dry mass vertical coordinate is defined in section 2.4. more details on other sections

2.1 Representation of water phases in terms of dry and wet (specific) mixing ratios

Define the dry mixing ratios for the water variables (dry air 'd', water vapor 'vw', cloud liquid 'cl' and cloud ice 'ci')

$$m^{(\ell)} \equiv \frac{\rho^{(\ell)}}{\rho^{(d)}}, \text{ where } \ell = `d`, `wv`, `cl`, `ci`, \tag{1}$$

where $\rho^{(d)}$ is the mass of dry air per unit volume of moist air and $\rho^{(\ell)}$ is the mass of the water substance of type ℓ per unit volume of moist air. By moist air we refer to air containing dry air, water vapor, cloud liquid and cloud ice. Note that the mixing ratio for dry air is one: $m^{(d)} \equiv \frac{\rho^{(d)}}{\rho^{(d)}} = 1$.

Similarly define moist (or, equivalently, specific) mixing ratios

$$q^{(\ell)} \equiv \frac{\rho^{(\ell)}}{\sum_\ell \rho^{(\ell)}}, \text{ where } \ell = \text{‘}wv\text{‘}, \text{‘}cl\text{‘}, \text{‘}ci\text{‘}. \tag{2}$$

where, in particular, $q^{(wv)}$ is the specific humidity. The sum on the right-hand side denominator of (2), $\sum_\ell$, is over dry air density and the density of all water variables (ℓ = ‘d‘, ‘wv‘, ‘cl‘, ‘ci‘’). The derivations below can easly be extended to include more water variables. We will use this notation throughout the paper.

One can convert between moist and dry mixing ratios easily

$$m^{(\ell)} = \frac{q^{(\ell)}}{1 + q^{(d)} - \sum_\ell q^{(\ell)}}, \tag{3}$$

$$q^{(\ell)} = \frac{m^{(\ell)}}{\sum_\ell m^{(\ell)}}. \tag{4}$$

Note that if water vapor undergoes a phase change to rain and leaves the column, then the specific/wet mixing ratios change but the dry mixing ratio does not.

The density of a unit volume of moist air is related to the dry air density through

$$\rho = \rho^{(d)} \left(\sum_\ell m^{(\ell)} \right). \tag{5}$$

2.2 Ideal gas law and virtual temperature

In this section the ideal gas law is derived for moist air containing condensates. Part of that derivation is the definition of virtual temperature.

If we assume that moist air obeys Amagat’s law (or the law of partial volumes) then a unit volume of moist air $V = 1$ is the sum of the volumes of the different forms of water in the air

$$V = \sum_\ell V^{(\ell)}. \tag{6}$$

Now let $\alpha \equiv \frac{1}{\rho}$ denote the specific volume of moist air, let $\hat{\alpha}^{(gas)}$ be the specific volume of the gaseous components of moist air (the volume of water vapor and dry air per unit mass of water vapor and dry air), let $\hat{\alpha}^{(cl)}$ be the specific volume of cloud liquid (i.e. volume occupied by unit mass of cloud liquid), and similarly for cloud ice. Then we can write (6) in terms of densities and specific volumes

$$\rho\alpha = \rho^{(gas)}\hat{\alpha}^{(gas)} + \rho^{(cl)}\hat{\alpha}^{(cl)} + \rho^{(ci)}\hat{\alpha}^{(ci)}, \tag{7}$$

where $\rho^{(gas)} = \rho^{(d)} + \rho^{(wv)}$. Note that $\hat{\alpha}^{(\ell)} \neq \frac{1}{\rho^{(\ell)}}$ since $\rho^{(\ell)}$ is defined in terms mass of ℓ per unit volume of moist air and not mass of ℓ per unit volume of water phase ℓ. Dividing (7) with $\rho^{(d)}$ and substituting (1) yields

$$\left(\sum_\ell m^{(\ell)} \right) \alpha = \left(1 + m^{(wv)} \right) \hat{\alpha}^{(gas)} + m^{(cl)}\hat{\alpha}^{(cl)} + m^{(ci)}\hat{\alpha}^{(ci)}. \tag{8}$$

The ideal gas law for the gaseous components, using Dalton’s law of partial pressures, is

$$p = p^{(d)} + p^{(wv)} = \rho^{(d)} R^{(d)} T + \rho^{(wv)} R^{(wv)} T, \tag{9}$$

where $p^{(d)}$ is the dry pressure and $p^{(wv)}$ is the water vapor pressure. We may write (9) in terms of $\rho^{(gas)}$ by multiplying (9) with $\frac{\rho^{(gas)}}{\rho^{(gas)}}$ and write the equation in terms of mixing ratios

$$p = \rho R^{(d)} T \rho^{(gas)} \left(\frac{\rho^{(d)}}{\rho^{(gas)}} + \frac{\rho^{(wv)}}{\rho^{(gas)}} \frac{R^{(wv)}}{R^{(d)}} \right) = \frac{R^{(d)} \rho^{(gas)} T \left(1 + \frac{1}{\epsilon} m^{(wv)} \right)}{\left(1 + m^{(wv)} \right)}. \tag{10}$$

where $\epsilon \equiv \frac{R^{(d)}}{R^{(wv)}}$. Since (9) holds for the gaseous components only we may substitute $\frac{1}{\rho^{(gas)}}$ with $\hat{\alpha}^{(gas)}$ to get:

$$p = \frac{R^{(d)} T \left(1 + \frac{1}{\epsilon} m^{(wv)}\right)}{\left(1 + m^{(wv)}\right) \hat{\alpha}^{(gas)}}. \tag{11}$$

Using (8) to eliminate $\left(1 + m^{(wv)}\right) \hat{\alpha}^{(gas)}$ in (11) and simplifying yields

$$p = \rho R^{(d)} T_v, \tag{12}$$

where the virtual temperature is given by

$$T_v = T \left[\frac{1 + \frac{1}{\epsilon} m^{(wv)}}{1 + m^{(wv)} + m^{(cl)} \left(1 - \frac{\hat{\alpha}^{(cl)}}{\alpha}\right) + m^{(ci)} \left(1 - \frac{\hat{\alpha}^{(ci)}}{\alpha}\right)} \right]. \tag{13}$$

The ratio of the density of moist air to the density of cloud liquid and cloud ice is negligible (the terms $\frac{\hat{\alpha}^{(cl)}}{\alpha}$ and $\frac{\hat{\alpha}^{(cl)}}{\alpha}$ are of order 10^{-3} or less) hence the formula for virtual temperature is simplified to

$$T_v = T \left(\frac{1 + \frac{1}{\epsilon} m^{(wv)}}{\sum_i m^{(\ell)}} \right). \tag{14}$$

2.3 Thermodynamic equation

The first law of thermodynamics for a mixture of dry air, water vapor, cloud liquid water and cloud ice is given by

$$\frac{\sum_\ell c_v^{(\ell)} m^{(\ell)}}{\sum_\ell m^{(\ell)}} \delta T + p \delta \alpha = \delta Q, \tag{15}$$

where δQ is the amount of heat per unit mass that is supplied reversibly to the moist air, δT and $\delta \alpha$ are the moist airs temperature and specific volume changes and $c_v^{(\ell)}$ is the heat capacity at constant volume for component ℓ of moist air. Note that

$$\begin{aligned}
\left(\sum_\ell m^{(\ell)}\right) p \delta \alpha &= p \delta \left[\left(\sum_\ell m^{(\ell)}\right) \alpha \right], && (16)\\
&= (1 + m^{(wv)}) p \delta \hat{\alpha}^{(gas)}, && (17)\\
&= \left(R^{(d)} + m^{(wv)} R^{(wv)}\right) \left(\delta T - \frac{T}{p} \delta p\right). && (18)
\end{aligned}$$

where, in (16), we have assumed that $m^{(\ell)}$ is constant. To get (17) we substituted (8) into the right-hand side of (16) and assumed that cloud ice and liquid are incompressible ($\delta \hat{\alpha}^{(cl)} = 0$ and $\delta \hat{\alpha}^{(ci)} = 0$). Finally (11) has been used to substitute for $\hat{\alpha}^{(gas)}$ in (18). Using (18) in the First law of thermodynamics (15), substituting $R^{(d)} = c_v^{(d)} - c_v^{(d)}$ and $R^{(wv)} = c_p^{(wv)} - c_v^{(wv)}$, using that $c_p^{(\ell)} = c_v^{(\ell)}$ for cloud liquid and ice (since they are incompressible) and rearranging terms yields

$$\delta T - \frac{\left(R^{(d)} + m^{(wv)} R^{(wv)}\right)}{\left(\sum c_p^{(\ell)} m^{(\ell)}\right)} \frac{T}{p} \delta p = \frac{\left(\sum_\ell m^{(\ell)}\right)}{\left(\sum_\ell c_p^{(\ell)} m^{(\ell)}\right)} \frac{\delta Q}{T}. \tag{19}$$

Equation (19) can be written in a more familiar form

$$\delta T - \frac{R}{c_p} \frac{T}{p} \delta p = \frac{1}{c_p T} \delta Q, \tag{20}$$

if we define c_p and R as

$$\begin{aligned}
c_p &= \frac{\sum_\ell c_p^{(\ell)} m^{(\ell)}}{\sum_\ell m^{(\ell)}}, && (21)\\
R &= \frac{\sum_\ell R^{(\ell)} m^{(\ell)}}{\sum_\ell m^{(\ell)}}. && (22)
\end{aligned}$$

where $R^{(cl)} = 0$ and $R^{(ci)} = 0$. Note that with these definitions of c_p and R the ideal gas law can be written as

$$p = \rho R T, \tag{23}$$

and

$$c_p = R + c_v. \tag{24}$$

The thermodynamic equation (20) may also be written in terms of full density

$$\delta T - \frac{1}{\rho\, c_p}\delta p = \frac{1}{c_p T}\delta Q. \tag{25}$$

2.4 Vertical coordinate

2.4.1 Definition

Let $\mathcal{P}_s^{(d)}$ be the surface pressure of a dry atmosphere and $\mathcal{P}_t^{(d)}$ the pressure at the model top. We assume that there is no moisture or condensate above the model top so $p_t^{(d)} = p_t^{(wv)} = \mathcal{P}_t^{(d)}$. Consider a general, terrain-following, vertical coordinate $\eta^{(d)}$ that is a function of dry atmosphere pressure $\mathcal{P}^{(d)}$

$$\eta^{(d)} = h(\mathcal{P}^{(d)}, \mathcal{P}_s^{(d)}), \tag{26}$$

where $h(\mathcal{P}s^{(d)}, \mathcal{P}s^{(d)}) = 1$ and $h(\mathcal{P}t^{(d)}, \mathcal{P}s^{(d)}) = 0$. Note that by removing the superscript (d) from the equations above so that the dry variable represent moist pressure variables then the vertical coordinate is the usual hybrid-pressure coordinate widely used in hydrostatic global modeling [*Simmons and Burridge*, 1981]. The top and bottom boundary conditions are that $\dot{\eta}\left(\mathcal{P}s^{(d)}, \mathcal{P}s^{(d)}\right) = 0$ and $\dot{\eta}\left(\mathcal{P}t^{(d)}, \mathcal{P}s^{(d)}\right) = 0$. Note that using a dry-mass vertical coordinate simplifies the coupling to physics since the dry mass coordinates do not change location if there are water-vapor (or other phase changes) in the column.

2.4.2 Dry pressure and dry atmosphere pressure

The observant reader will have noticed that we denote the dry atmosphere pressure $\mathcal{P}^{(d)}$ and not $p^{(d)}$. The moist pressure at given height z' can be computed from the hydrostatic balance

$$
\begin{aligned}
p &= \int_{z'=z}^{z'=\infty} \rho\, g\, dz', &(27)\\
&= \int_{z'=z}^{z'=\infty} \rho_d \left(\sum_{\ell} m_\ell\right) g\, dz', &(28)\\
&= \sum_{\ell} \mathcal{P}^{(\ell)}, &(29)
\end{aligned}
$$

where the right-hand side of (29) is the weight of dry air, water vapor, cloud liquid and cloud ice per unit area, respectively:

$$\mathcal{P}^{(\ell)} = \int_{z'=z}^{z'=\infty} \rho_d\, m_\ell\, g\, dz'. \tag{30}$$

Using Dalton's law of partial pressures, (29) can be written as

$$p^{(d)} + p^{(wv)} = \sum_{\ell} \mathcal{P}^{(\ell)}. \tag{31}$$

From (31) it is clear that in the presence of condensate one can not equate $p^{(d)}$ with $\mathcal{P}^{(d)}$ and equate $p^{(wv)}$ with $\mathcal{P}^{(wv)}$. The dry pressure and water vapor pressure are both affected by the weight of the condensates even though the condensates do not exert a pressure. Hence the dry pressure $p^{(d)}$ is different from the pressure in a dry atmosphere $\mathcal{P}^{(d)}$ =

$\mathcal{P}^{(d)}$. The hydrostatic balance of a dry atmosphere, written in terms of differentials, is given by

$$d\mathcal{P}^{(d)} = -\rho_d g dz, \tag{32}$$

whereas, in a moist atmosphere, a dry pressure hydrostatic equation does not hold

$$dp^{(d)} \neq -\rho_d g dz. \tag{33}$$

The differential of the moist pressure can be written in terms of the dry atmosphere pressure though:

$$dp = -\rho g\, dz = -\rho_d \left(\sum_\ell m_\ell\right) g\, dz = d\mathcal{P}^{(d)} \left(\sum_\ell m_\ell\right). \tag{34}$$

2.5 Equations of motion

The $\eta^{(d)}$-coordinate adiabatic and frictionless atmospheric primitive equations assuming floating Lagrangian vertical coordinates [*Starr*, 1945; *Lin*, 2004] can be written as

$$\frac{\partial \vec{v}}{\partial t} + (\zeta + f)\,\hat{\vec{k}} \times \vec{v} + \nabla_{\eta^{(d)}} \left(\frac{1}{2}\vec{v}^2 + \Phi\right) + \frac{1}{\rho}\nabla_{\eta^{(d)}} p = 0, \tag{35}$$

$$\frac{\partial T}{\partial t} + \vec{v} \cdot \nabla_{\eta^{(d)}} T - \frac{1}{c_p \rho}\omega = 0, \tag{36}$$

$$\frac{\partial}{\partial t}\left(\frac{\partial \mathcal{P}^{(d)}}{\partial \eta^{(d)}} m^{(\ell)}\right) + \nabla_{\eta^{(d)}} \cdot \left(\frac{\partial \mathcal{P}^{(d)}}{\partial \eta^{(d)}} m^{(\ell)} \vec{v}\right) = 0, \quad \ell = \text{`}d\text{`}, \text{`}wv\text{`}, \text{`}cl\text{`}, \text{`}ci\text{`}, \tag{37}$$

where ρ is the full density $\sum_\ell \rho^{(\ell)}$, p is moist pressure, Φ is the geopotential height ($\Phi = g\,z$, where g is the gravitational constant), $\hat{\vec{k}}$ is the unit vector normal to the surface of the sphere, $\zeta = \hat{\vec{k}} \cdot \nabla \times \vec{v}$ is vorticity, f Coriolis parameter, and $\omega = Dp/Dt$ is the pressure vertical velocity.

The prognostic equations for $\vec{v}$, the temperature T, pseudo density of a dry atmpshere $\frac{\partial \mathcal{P}^{(d)}}{\partial \eta^{(d)}}$, and pseudo tracer density $\frac{\partial \mathcal{P}^{(d)}}{\partial \eta^{(d)}} m^{(\ell)}$ are solved with the diagnostic equation for geopotential height (hydrostatic balance)

$$\frac{\partial \Phi}{\partial \eta^{(d)}} = -\frac{R^{(d)}\, T_v}{p}\frac{\partial p}{\partial \eta^{(d)}}, \tag{38}$$

where

$$\frac{\partial p}{\partial \eta^{(d)}} = \frac{\partial \mathcal{P}^{(d)}}{\partial \eta^{(d)}}\left(\sum_\ell m^{(\ell)}\right). \tag{39}$$

For diagnosing vertical pressure velocity ω we note that

$$\omega(\eta^{(d)}) = \frac{dp}{dt}(\eta^{(d)}), \tag{40}$$

$$= \int_{\eta^{(d)}}^{\eta^{(d)}=0} \frac{d}{dt}\left(\frac{\partial p}{\partial \eta^{(d)}}\right) d\eta^{(d)}, \tag{41}$$

$$= \int_{\eta^{(d)}}^{\eta^{(d)}=0} \frac{\partial}{\partial t}\left(\frac{\partial p}{\partial \eta^{(d)}}\right) d\eta^{(d)} + \int_{\eta^{(d)}}^{\eta^{(d)}=0} \vec{v} \cdot \nabla \left(\frac{\partial p}{\partial \eta^{(d)}}\right) d\eta^{(d)}. \tag{42}$$

2.6 Hyperviscosity and frictional heating

2.6.1 Viscosity operator

The spectral-element method does not have implicit diffusion hence hyperviscosity operators are applied to the prognostic variables [Taylor reference]. On the right-hand side of the momentum equations (35) viscous terms $\nu\nabla^4\left(\nabla\times\vec{v}\right)+\nu_{div}\nabla^4\left(\nabla\cdot\vec{v}\right)$ are added. The velocity field is split into vorticity and divergence to allow for increased damping of divergent modes. The pseudo-density and temperature are damped with $\nu\nabla^4\left\{\frac{\partial p}{\partial\eta^{(d)}}\right\}$ and $\nu\nabla^4 T$. The horizontal hyperviscosity operator can be applied on η_d-surfaces, $\nu\nabla^4=\nu\nabla^4_{\eta_d}$, but it may be advantageous to apply the hyperviscosity operator on approximate pressure surfaces

$$\nu\nabla^4\Xi=\nu\nabla^4_{\eta_d}-\frac{\partial\Xi}{\partial p}\nu\nabla^4_{\eta_d}p,\qquad \Xi=\vec{v},T, \tag{43}$$

[p.58 in *Neale et al.*, 2010] to reduce spurious diffusion over steep topography.

2.6.2 Reference pressure damping

Patrick

2.6.3 Frictional heating

Let the $\delta\vec{v}$ be the change in the velocity vector due to diffusion of momentum. Then the change in kinetic energy due hyperviscosity applied to $\vec{v}$ is $\frac{1}{2}\rho\vec{v}\cdot\delta\vec{v}$. This kinetic energy is converted to a heating rate by adding a heating term $\delta\mathcal{T}$ in the thermodynamic equation corresponding to the kinetic energy change

$$\rho c_p\delta\mathcal{T}=-\frac{1}{2}\rho\vec{v}\cdot\delta\vec{v}\Rightarrow\delta\mathcal{T}=-\frac{1}{c_p}\left(\vec{v}\cdot\delta\vec{v}\right), \tag{44}$$

[p.71 in *Neale et al.*, 2010]. As shown in the results section this term is rather large and therefore important for good energy conservation characteristics of the dynamical core.

2.7 Global conservation

Below we show that the continuous equations of motion that include the effect of condensates conserve axial angular momentum and total energy. For the derivation below we first note that adding the continuity equations ℓ = 'd', 'wv', 'cl', 'ci' (37), using hydrostatic balance (38) and ideal gas law (12), the continuity equation for moist air can be written as

$$\frac{\partial}{\partial t}\left[\rho\left(\frac{\partial z}{\partial\eta^{(d)}}\right)\right]+\nabla_{\eta^{(d)}}\cdot\left[\vec{v}\rho\left(\frac{\partial z}{\partial\eta^{(d)}}\right)\right]=0, \tag{45}$$

or, equivalently, in Lagrangian form

$$\frac{D}{Dt}\left[\rho\left(\frac{\partial z}{\partial\eta^{(d)}}\right)\delta A\right]=0, \tag{46}$$

where δA is a horizontal area of a Lagrangian air parcel so that $\nabla\cdot\vec{v}=\frac{1}{\delta A}\frac{D}{Dt}\left(\delta A\right)$, and $\frac{D}{Dt}=\frac{\partial}{\partial t}+\vec{v}\cdot\nabla$ is the material/total derivative.

2.7.1 Axial angular momentum

The conservation law for angular momentum is derived in spherical coordinates for which the zonal momentum equation takes the form

$$\frac{Du}{Dt}=\frac{uv\tan\varphi}{r}+2\Omega v\sin\varphi-\frac{1}{\rho r\cos\varphi}\frac{\partial p}{\partial\lambda}, \tag{47}$$

where u and v the zonal and meridional velocity components, respectively, φ is latitude and λ longitude, Ω rotation rate of Earth ($f=2\Omega\sin\varphi$), and r is the mean radius of Earth.

The conservation law for axial angular momentum, $M=\left(u+\Omega r\cos\varphi\right)r\cos\varphi$, can be conveniently derived using the Lagrangian form. Consider the material derivative of M

multiplied by the volume of a Lagrangian air parcel, $\rho\left(\frac{\partial z}{\partial\eta^{(d)}}\right)\delta A$

$$\frac{D}{Dt}\left[\rho\left(\frac{\partial z}{\partial\eta^{(d)}}\right)\delta A\,(u+\Omega r\cos\varphi)\,r\cos\varphi\right]. \tag{48}$$

Using the chain rule, continuity equation on the form (46), the equality $v = r\frac{D\varphi}{Dt}$ and substituting (47), one can obtain an evolution equation for axial angular momentum

$$\frac{D}{Dt}\left[\rho\left(\frac{\partial z}{\partial\eta^{(d)}}\right)\delta A\,M\right] = -\left(\frac{\partial z}{\partial\eta^{(d)}}\right)\frac{\partial p}{\partial\lambda}, \tag{49}$$

or, equivalently, in Eulerian form

$$\frac{\partial}{\partial t}\left[\rho\left(\frac{\partial z}{\partial\eta^{(d)}}\right)M\right] + \nabla_{\eta_d}\cdot\left[\vec{v}\rho\left(\frac{\partial z}{\partial\eta^{(d)}}\right)M\right] = -\left(\frac{\partial z}{\partial\eta^{(d)}}\right)\frac{\partial p}{\partial\lambda}. \tag{50}$$

Repeatedly using the chain rule one can show that the right-hand side of (49) and (50) can be written as

$$-\left(\frac{\partial z}{\partial\eta^{(d)}}\right)\frac{\partial p}{\partial\lambda} = -\frac{\partial}{\partial\lambda}\left[\left(\frac{\partial z}{\partial\eta^{(d)}}\right)p\right] + p\frac{\partial}{\partial\lambda}\left(\frac{\partial z}{\partial\eta^{(d)}}\right) \tag{51}$$

$$= -\frac{\partial}{\partial\eta^{(d)}}\left(\frac{\partial z}{\partial\lambda}p\right) + \left(\frac{\partial z}{\partial\eta^{(d)}}\right)\frac{\partial p}{\partial\lambda} + p\frac{\partial}{\partial\lambda}\left(\frac{\partial z}{\partial\eta^{(d)}}\right), \tag{52}$$

$$= -\frac{\partial}{\partial\eta^{(d)}}\left(\frac{\partial z}{\partial\lambda}p\right) + \left(\frac{\partial z}{\partial\eta^{(d)}}\right)\frac{\partial p}{\partial\lambda} - \frac{\partial}{\partial\lambda}\left[p\left(\frac{\partial z}{\partial\eta^{(d)}}\right)\right] - \frac{\partial p}{\partial\lambda}\left(\frac{\partial z}{\partial\eta^{(d)}}\right). \tag{53}$$

$$= -\frac{\partial}{\partial\eta^{(d)}}\left(\frac{\partial z}{\partial\lambda}p\right) - \frac{\partial}{\partial\lambda}\left[p\left(\frac{\partial z}{\partial\eta^{(d)}}\right)\right]. \tag{54}$$

Substituting (54) on the right-hand side of (50) and integrating (50) in the vertical we get

$$\frac{\partial}{\partial t}\int_{\eta=0}^{\eta=1}\left[\left(\sum_{\ell}m^{(\ell)}\right)\left(\frac{\partial\mathcal{P}^{(d)}}{\partial\eta^{(d)}}\right)M\right]d\eta^{(d)} + \nabla_{\eta_d}\cdot\int_{\eta=0}^{\eta=1}\left[\vec{v}M\right]d\eta^{(d)} = -\left(\frac{\partial z}{\partial\eta^{(d)}}\right)\frac{\partial p}{\partial\lambda}. \tag{55}$$

2.7.2 Total energy

The derivation of the total energy equation closely follows *Kasahara* [1974] but for a dry mass vertical coordinate and inclusion of condensates in the equations of motion. The equation for the horizontal kinetic energy per unit mass, $K = \frac{1}{2}\vec{v}\cdot\vec{v}$, is derived by multiplying the momentum equations (35) with $\rho\vec{v}\left(\frac{\partial z}{\partial\eta^{(d)}}\right)$ and the continuity equation (45) with K, adding the two resulting equations and simplifying using the chain rule yields

$$\frac{\partial}{\partial t}\left[\rho\left(\frac{\partial z}{\partial\eta^{(d)}}\right)K\right] + \nabla_{\eta^{(d)}}\left[\rho\vec{v}\left(\frac{\partial z}{\partial\eta^{(d)}}\right)K\right] = -\left(\frac{\partial z}{\partial\eta^{(d)}}\right)\vec{v}\nabla_{\eta^{(d)}}p - g\rho\left(\frac{\partial z}{\partial\eta^{(d)}}\right)\vec{v}\cdot\nabla_{\eta^{(d)}}z. \tag{56}$$

For the derivation of a flux-form version of the total energy equation (that includes the a geopotential term) we substitute

$$g\rho\left(\frac{\partial z}{\partial\eta^{(d)}}\right)\vec{v}\cdot\nabla_{\eta^{(d)}}z = \nabla_{\eta^{(d)}}\cdot\left[gz\vec{v}\rho\left(\frac{\partial z}{\partial\eta^{(d)}}\right)\right] - gz\nabla_{\eta^{(d)}}\cdot\left[\vec{v}\rho\left(\frac{\partial z}{\partial\eta^{(d)}}\right)\right], \tag{57}$$

$$= \nabla_{\eta^{(d)}}\cdot\left[gz\vec{v}\rho\left(\frac{\partial z}{\partial\eta^{(d)}}\right)\right] - z\nabla_{\eta^{(d)}}\cdot\left[\vec{v}\left(\frac{\partial p}{\partial\eta^{(d)}}\right)\right], \tag{58}$$

(where the hydrostatic balance equation (38) has been used on the right-hand side of (58)) on the right-hand side of (56) and rearranging terms:

$$\frac{\partial}{\partial t}\left[\rho\left(\frac{\partial z}{\partial\eta^{(d)}}\right)K\right] + \nabla_{\eta^{(d)}}\cdot\left[\rho\vec{v}\left(\frac{\partial z}{\partial\eta^{(d)}}\right)(K+gz)\right] = -\left(\frac{\partial z}{\partial\eta^{(d)}}\right)\vec{v}\nabla_{\eta^{(d)}}p - z\nabla_{\eta^{(d)}}\cdot\left[\vec{v}\left(\frac{\partial p}{\partial\eta^{(d)}}\right)\right]. \tag{59}$$

Now, by multiplying the thermodynamic equation (36) with $\rho\frac{\partial z}{\partial\eta^{(d)}}c_p$ and the continuity equation (45) with c_pT, adding the resulting equations and simplifying using the chain rule yields

$$\frac{\partial}{\partial t}\left[\rho\left(\frac{\partial z}{\partial\eta^{(d)}}\right)c_pT\right]+\nabla_{\eta^{(d)}}\left[\rho\vec{v}\left(\frac{\partial z}{\partial\eta^{(d)}}\right)c_pT\right]=\left(\frac{\partial z}{\partial\eta^{(d)}}\right)\omega. \tag{60}$$

By using that $\omega\equiv\frac{\partial p}{\partial t}+\vec{v}\cdot\nabla_{\eta^{(d)}}p$, using the chain rule and the continuity equation (45) , one can show that

$$\left(\frac{\partial z}{\partial\eta^{(d)}}\right)\omega=\frac{\partial}{\partial\eta^{(d)}}\left(z\frac{\partial p}{\partial t}\right)+\left(\frac{\partial z}{\partial\eta^{(d)}}\right)\vec{v}\nabla_{\eta^{(d)}}p+z\nabla_{\eta^{(d)}}\cdot\left[\vec{v}\frac{\partial p}{\partial\eta^{(d)}}\right]. \tag{61}$$

Substituting (61) on the right-hand side of (60) and adding the resulting equation to (59), the two terms on the right-hand side of (59) cancel the two last terms on the right-hand side of (61) and we get the total energy equation

$$\frac{\partial}{\partial t}\left[\rho\left(\frac{\partial z}{\partial\eta^{(d)}}\right)\left(K+c_pT\right)\right]+\nabla_{\eta^{(d)}}\left[\rho\vec{v}\left(\frac{\partial z}{\partial\eta^{(d)}}\right)\left(K+gz+c_pT\right)\right]=\frac{\partial}{\partial\eta^{(d)}}\left(z\frac{\partial p}{\partial t}\right). \tag{62}$$

This equation has the form as (5.7) in *Kasahara* [1974] but ρ, c_p and p include the effect of condensates. Noting that

$$c_pT\rho\left(\frac{\partial z}{\partial\eta^{(d)}}\right)=c_vT\rho\left(\frac{\partial z}{\partial\eta^{(d)}}\right)+gz]\rho\left(\frac{\partial z}{\partial\eta^{(d)}}\right), \tag{63}$$

where we have used the ideal gas law on the form (23), chain rule and hydrostatic equation on the form (38), the total energy equation can be written on the form

$$\frac{\partial}{\partial t}\left[\rho\left(\frac{\partial z}{\partial\eta^{(d)}}\right)(K+c_vT+gz)\right]+\nabla_{\eta^{(d)}}\left[\rho\vec{v}\left(\frac{\partial z}{\partial\eta^{(d)}}\right)\left(K+gz+c_pT\right)\right]=-\frac{\partial}{\partial\eta^{(d)}}\left(p\frac{\partial z}{\partial t}\right). \tag{64}$$

As an aside it is noted that a z-based vertical coordinate (for a moment assume $\eta^{(d)}\equiv z$), then integrating (64) in the vertical and using that z is constant at the model top (z_{top}) and surface (z_s) we get

$$\frac{\partial}{\partial t}\int_{z=z_s}^{z=z_{top}}(K+c_vT+gz)\,\rho dz+\nabla_z\cdot\int_{z=z_s}^{z=z_{top}}\vec{v}\left(K+gz+c_pT\right)\rho dz=0, \tag{65}$$

we get a clear separation of kinetic (K), potential (gz) and internal (c_vT) energy. Integrating (65) in the horizontal over the entire sphere the flux term drops out, and it is clear that the total energy is conserved for the frictionless and adiabatic system of equations.

For the global integral of the total energy equation in a dry-mass vertical coordinate, we substitute the hydrostatic relation on the form (38) into (62), integrate in the vertical and use that the pressure at the model top is constant,

$$\begin{aligned}\frac{1}{g}\frac{\partial}{\partial t}\int_{\eta=0}^{\eta=1}\left(\sum_\ell m^{(\ell)}\right)\left(\frac{\partial\mathcal{P}^{(d)}}{\partial\eta^{(d)}}\right)\left(K+c_pT\right)d\eta^{(d)}&\\ +\frac{1}{g}\nabla_{\eta^{(d)}}\cdot\int_{\eta=0}^{\eta=1}\vec{v}\left(\sum_\ell m^{(\ell)}\right)\left(\frac{\partial\mathcal{P}^{(d)}}{\partial\eta^{(d)}}\right)\left(K+gz+c_pT\right)d\eta^{(d)}&=-z_s\frac{\partial p_s}{\partial t},\end{aligned} \tag{66}$$

which can also be written as

$$\begin{aligned}\frac{1}{g}\frac{\partial}{\partial t}\int_{\eta=0}^{\eta=1}\left(\frac{\partial\mathcal{P}^{(d)}}{\partial\eta^{(d)}}\right)\sum_\ell\left[m^{(\ell)}\left(K+c_p^{(\ell)}T+\Phi_s\right)\right]d\eta^{(d)}&\\ +\frac{1}{g}\nabla_{\eta^{(d)}}\cdot\int_{\eta=0}^{\eta=1}\vec{v}\left(\frac{\partial\mathcal{P}^{(d)}}{\partial\eta^{(d)}}\right)\sum_\ell\left[m^{(\ell)}\left(K+c_p^{(\ell)}T+gz\right)\right]d\eta^{(d)}&=0.\end{aligned} \tag{67}$$

by expanding c_p using (21), re-arranging terms and using that $\Phi_s = gz_s$ is time-independent and that

$$p_s = \int_{\eta=0}^{\eta=1} \sum_{\ell} \left(\frac{\partial \mathcal{P}^{(d)}}{\partial \eta^{(d)}} \right) m^{(\ell)} d\eta^{(\eta)}. \tag{68}$$

Note that the energy terms (inside square brackets) in (67) separate into dry air, water vapor, cloud liquid and cloud ice componets

$$\left(\frac{\partial \mathcal{P}^{(d)}}{\partial \eta^{(d)}} \right) \sum_{\ell} \left[m^{(\ell)} \left(K + c_p^{(\ell)} T + \Phi_s \right) \right]. \tag{69}$$

Similarly for the flux term in the second square brackets on the left-hand side of (67). Integrating (67) over the entire sphere results in

$$\frac{1}{g} \frac{\partial}{\partial t} \int_{\eta=0}^{\eta=1} \iint \left(\frac{\partial \mathcal{P}^{(d)}}{\partial \eta^{(d)}} \right) \sum_{\ell} \left[m^{(\ell)} \left(K + c_p^{(\ell)} T + \Phi_s \right) \right] r \, d\lambda \, d\varphi d\eta^{(d)} = 0. \tag{70}$$

We note that the CAM physics package energy fixer assumes that the 'perfect' adiabatic dynamical core conserves an energy where $c_p^{(vw)} = c_p^{(d)}$, $c_p^{(\ell)} = 0$ for ℓ = 'cl', 'ci' and $m^{(\ell)} = 0$ for ℓ = 'cl', 'ci' [*Williamson et al.*, 2015]. In other words, the CAM energy fixer uses a dry total energy. The discrepancy between the more comprehensive energy formula (70) and the CAM physics formula for total energy is about 0.5 W/m^2 [*Taylor*, 2011].

3 Discretized equations of motion

3.1 Vertical discretization

In the vertical the atmosphere is discretized into $nlev$ floating Lagrangian layers. The vertical index is 1 for the upper most level and $nlev$ in the lower most level. The level interfaces are referred to as half-levels so that layer k is bounded by interface level $k + 1/2$ and $k - 1/2$. Since we are using a dry-mass vertical reference coordinate, the dry atmosphere reference pressure at the layer interfaces is defined in terms of the hybrid coefficients A and B that are only a function of level index

$$\mathcal{P}_{k+1/2}^{(d)} = A_{k+1/2} p_t + B_{k+1/2} \mathcal{P}_s^{(d)}, \tag{71}$$

and similartly for full levels k. Note that if the 'd' is removed from the above equation so that the levels are based on moist pressure then the vertical coordinate reduces to the usual hybrid vertical coordinate used in many global hydrostatic models. Every $rsplit$ time-steps the floating Lagrangian levels the prognostic variables are remapped to the dry-mass reference coordinate (71) (see Section 3.1.5).

CAM-SE is based on a Lorenz vertical staggering so the full level prognostic variables are $\vec{v}_k$ (velocity vector), T_k (temperature), $\Delta\mathcal{P}_k^{(d)} = \mathcal{P}_{k+1/2}^{(d)} - \mathcal{P}_{k-1/2}^{(d)}$ (dry atmosphere pressure level thickness), and $\Delta\mathcal{P}_k^{(d)} m_k^{(\ell)}$ (tracer mass). At the level interfaces we have geopotential, pressure, vertical velocity and density. In the equations of motion the full level pressure, geopotential height, vertical velocity and density are needed and choices must be made on how these variables are derived (in discretized space) from the prognostic variables. Here we use the energy and angular momentum conserving method of *Simmons and Burridge* [1981] to compute these quantities at full levels as discussed in the sections below.

For simplicity we do not discretize in the horizontal [some wording about spectral element method in the horizontal needed ....]

3.1.1 Pressure

The half-level moist pressure is

$$p_{k+1/2} = p_t + \sum_{j=1}^{nlev} \Delta\mathcal{P}_j^{(d)} \left(\sum_\ell m_j^{(\ell)} \right), \tag{72}$$

where p_t is the pressure at the model top, $\eta^{(d)} = 0$. The full level moist pressure is obtained by averaging [*Simmons and Burridge*, 1981]

$$p_k = \frac{p_{k+1/2} + p_{k-1/2}}{2}. \tag{73}$$

3.1.2 Geopotential height

Discretizing (38) in the vertical yields

$$\Phi_{k+1/2} = \Phi_s + R^{(d)} \sum_j \left(\frac{T_k}{p_k} \right) \Delta p_j, \tag{74}$$

where the full pressure p_k is computed as described in section 3.1.1. The half level geopotential is computed by averaging

$$\Phi_k = \frac{\Phi_{k+1/2} + \Phi_{k-1/2}}{2}. \tag{75}$$

3.1.3 Vertical pressure velocity

The vertical pressure velocity ω is obtained by discretizing (42). The first term on the right-hand side of (42) can be computed by using the continuity equations for dry pressure level thickness and water vapor mass in each layer (37)

$$\frac{\partial}{\partial t} \left[\sum_{j=1}^{k} \Delta\mathcal{P}_j^{(d)} \left(\sum_\ell m_j^{(\ell)} \right) \right] = - \sum_{j=1}^{k} \nabla_{\eta^{(d)}} \cdot \left[\Delta\mathcal{P}_j^{(d)} \left(\sum_\ell m_j^{(\ell)} \right) \right], \tag{76}$$

so that the vertical pressure velocity at half-levels is given by

$$\omega_{k+1/2} = - \sum_{j=1}^{k} \nabla_{\eta^{(d)}} \cdot \left[\Delta\mathcal{P}_j^{(d)} \left(\sum_\ell m_j^{(\ell)} \right) \right] + \sum_{j=1}^{k} \vec{v}_k \cdot \nabla_{\eta^{(d)}} \left[\Delta\mathcal{P}_j^{(d)} \left(\sum_\ell m_j^{(\ell)} \right) \right], \tag{77}$$

and full level ω is

$$\omega_k = \frac{\omega_{k+1/2} + \omega_{k-1/2}}{2}. \tag{78}$$

3.1.4 Density

Full level density is computed from the ideal gas law (12)

$$\rho_k = \frac{p_k}{R^{(d)} T_k^{(v)}}, \tag{79}$$

where the full pressure p_k is computed as described in section 3.1.1. The virtual temperature is based on prognostic variables defined at the layer centers so simple substitution into (14) yields $T_k^{(v)}$. Similarly for the computation of $\left(c_p\right)_k$.

3.1.5 Vertical remapping

To avoid excessive deformation or even crossing of the floating Lagrangian levels the prognostic variables defined at

$$\mathcal{P}_{k+1/2}^{(d)} = p_t + \sum_{j=1}^{k} \Delta\mathcal{P}_j^{(d)}, \tag{80}$$

the prognostic variables are remapped back to the (Eulerian) reference levels given in (71) every *rsplit* time-steps. In the remapping process we enforce conservation of mass by mapping $m_k^{(\ell)}\Delta\mathcal{P}_k^{(d)}$ using the piecewise-parabolic method [PPM; *Colella and Woodward*, 1984] and applying a standard shape-preserving limiter to avoid unphysical (in particular negative) mixing ratios in the remapping process. The internal energy is also conserved during the remapping process by mapping $\sum_\ell c_p^{(\ell)} m^{(\ell)} T_k \Delta\mathcal{P}_k^{(d)}$. Note that temperature must be recovered from the internal energy using the remapped tracer values for $m^{(\ell)}$. A shape-preserving filter is also used for the remapping of internal energy so that an isothermal profile remains isothermal if the limiter is active on one of the $m^{(\ell)}$. Note that if the limiter is active at the same points for more than one of the water species then we can not guarantee preservation of an isothermal atmosphere [see, e.g., Section 2.5 in *Lauritzen and Thuburn*, 2012].

The moist mass-weighted velocity compenents, $\sum_\ell m^{(\ell)}\Delta\mathcal{P}_k^{(d)} u_k$ and $\sum_\ell m^{(\ell)}\Delta\mathcal{P}_k^{(d)} v_k$ respectively, are remapped seperately. Mapping the moist mass weighted velocity components conservatively leads to an angular momentum conserving vertical remapping algorithm.

3.2 Horizontal discretization

The CAM-SE uses cubed-sphere geometry originally introduced by *Sadourny* [1972] to represent the planet earth. The spherical surface $\mathcal{S}$ is a patched domain, which is partitioned into non-overlapping quadrilateral elements Ω_e such that $\mathcal{S} = \cup\Omega_e$ (see Fig. 1). On $\mathcal{S}$ each 2D element $\Omega_e(x^1, x^2)$ defined in terms of central (gnomonic) projection angles $x^1, x^2 \in [-\pi/4, \pi/4]$, which serve as the independent variables in the computational domain. The mapping from cube to sphere results in a non-orthogonal curvilinear coordinate system on $\mathcal{S}$, with the metric tensor G_{ij} and analytic Jacobian $\sqrt{G} = |G_{ij}|^{1/2}$, $i, j \in \{1, 2\}$. A physical vector quantity such as the wind vector $\mathbf{v} = (u, v)$, defined on $\mathcal{S}$ in orthogonal lat-long coordinates, can be uniquely expressed in tensor form using conventional notations as the covariant (u_1, u_2) and contravariant (u^1, u^2) vectors (see *Nair et al.* [2005] for details). The governing equations defined in familiar vector form can also be expressed in general tensor form. In order to describe the SE discretization process in simple terms, we consider the the flux form transport equation on $\mathcal{S}$ for an arbitrary scalar ϕ:

$$\frac{\partial\phi}{\partial t} + \nabla\cdot\mathbf{F}(\phi) = S(\phi) \quad \Rightarrow \frac{\partial U}{\partial t} + \nabla_h\cdot\mathbf{F}(U) = S(U), \tag{81}$$

with $U = \sqrt{G}\phi$, $\mathbf{F} = (F^1, F^2)$ contravariant fluxes and S(U) is an arbitrary source term, and the gradient $\nabla_h = (\partial/\partial x^1, \partial/\partial x^2)$ defined on computational domain C corresponding to $\mathcal{S}$ under the gnomonic mapping.

3.3 SE spatial discretization in 2D

The SE solution process involves casting the PDE in Galerkin form, i.e., by multiplying (81) with a test (weight) function ψ and integrating over the domain C,

$$\int_C \psi\left[\frac{\partial U}{\partial t} + \nabla_h\cdot\mathbf{F}(U) - S(U)\right] dC = 0. \tag{82}$$

A computational form of (82) is obtained by applying Green's theorem, resulting in the weak Galerkin form as follows:

$$\int_C \psi\,\frac{\partial U}{\partial t}\,dC = \int_C \nabla_h\psi\cdot\mathbf{F}(U)\,dC + \int_C \psi\,S(U)\,dC, \tag{83}$$

where the approximate solution U and the test function belong to a polynomial space V_N. The SE method consists of partitioning the domain into non-overlapping elements and solving the global problem locally on each element, where the solution is approximated by using a set of basis (polynomial) functions of prescribed order N. A basic assumption used in SE (or continuous Galerkin) method is that the global basis corresponding to (83) is C^0 continuous. Therefore the problem (83) can be solved locally for each element Ω_e, if there is a mechanism by which the solution maintains C^0 continuity at the element boundaries as required by the SE discretization.

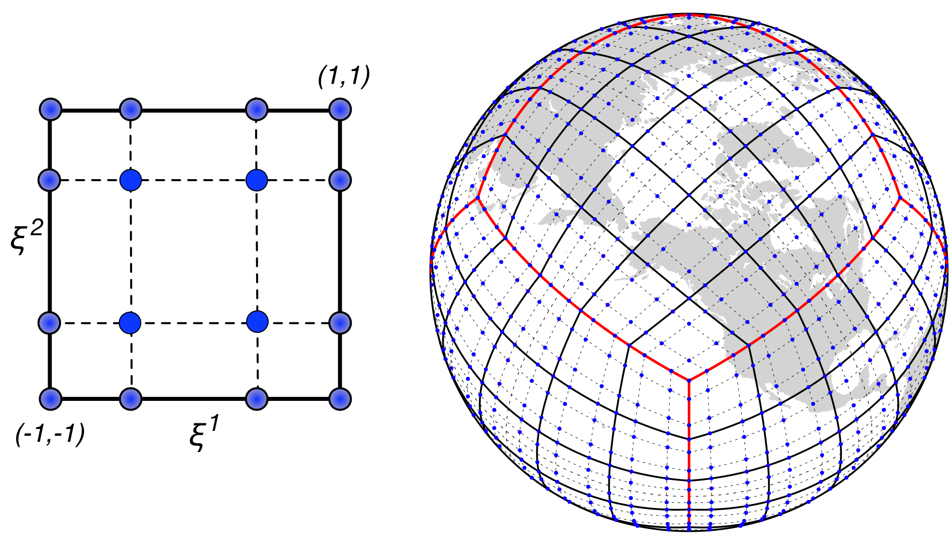

Figure 1. The left panel shows the Gauss-Lobatto-Legendre (GLL) grid with $N_v \times N_v$ quadrature points defined on a standard element $[-1,1]^2$, where $N_v = 4$. The right panel shows the cubed-sphere ($\mathcal{S}$) grid system tiled with $6N_e^2$ spectral elements Ω_e, where N_e is the number of elements in each coordinate direction on a panel. Each element Ω_e on $\mathcal{S}$ has the GLL grid structure.

For efficient evaluation of the integral equation (83), the SE method employs the Gauss-Lobatto-Legendre (GLL) quadrature rule for integrals and collocation differentiation for derivative operators. All the corresponding numerical operations are performed on a square $[-1,1]^2$ known as the standard (or reference) element. In order to facilitate local mesh refinement, the spectral elements Ω_e on $\mathcal{S}$ are defined as arbitrary spherical quadrilaterals in the CAM-SE grid system, which should be mapped onto the standard element. A direct way to address this problem is establishing a transformation $\mathcal{J}_e : \Omega_e \rightarrow [-1,1]^2$. $\mathcal{J}_e$ may be considered as a composite mapping combining the gnomonic and the quadrilateral to standard-element mapping. Let the Jacobian associated with the composite mapping be $J_e = J_e(\sqrt{G})$. Then an arbitrary surface integral on Ω_e can be expressed in terms of local coordinates $\xi^1, \xi^2 \in [-1,1]$ and the Jacobian J_e;

$$\int_{\Omega_e} \psi(x^1,x^2)\, d\Omega_e = \int_{-1}^{1}\int_{-1}^{1} J_e(\xi^1,\xi^2)\,\psi(\xi^1,\xi^2)\, d\xi^1\, d\xi^2 \approx \sum_{k=0}^{N}\sum_{l=0}^{N} w_k w_l\, J_e(\xi_k^1,\xi_l^2)\,\psi(\xi_k^1,\xi_l^2), \tag{84}$$

where w_k, w_l are the Gauss quadrature weights.

In the case of GLL quadrature rule, the nodal points ξ_k, $k = 0,1,\ldots,N$, are the roots of the polynomial $(1-\xi^2)P_N'(\xi) = 0$, $\xi \in [-1,1]$; and the corresponding GLL quadrature weights are given by

$$w_k = \frac{2}{N(N+1)\,[P_N(\xi_k)]^2},$$

where $P_N(\xi)$ is the Legendre polynomial of degree N. For the SE discretization it is customary to use Lagrange polynomials $h_k(\xi)$, with roots at the GLL quadrature points ξ_k, as basis functions. This setup provides discrete orthogonality for the basis function $h_k(\xi)$, which is formally defined as:

$$h_k(\xi) = \frac{(\xi^2 - 1)\, P'_N(\xi)}{N(N+1)\, P_N(\xi_k)\, (\xi - \xi_k)}. \tag{85}$$

Note that there are $N + 1 = N_v$ GLL quadrature points in 1D, and $N_v \times N_v$ GLL points are needed for 2D spectral elements Ω_e. Figure (1) shows the GLL grid with $N_v = 4$ on the left panel, and the right panel shows the cubed-sphere grid $\mathcal{S}$ tiled with elements Ω_e, each with the GLL grid points.

A semi-discrete form of (83) on an element Ω_e can by obtained by approximating the solution as a tensor product of 1D Lagrange basis $\{h_k(\xi)\}_{k=0}^{N}$ such that

$$U|_{\Omega_e} \approx U^e(\xi^1, \xi^2, t) = \sum_{k=0}^{N} \sum_{l=0}^{N} U^e_{kl}(t)\, h_k(\xi^1)\, h_l(\xi^2), \tag{86}$$

where $U^e_{kl}(t) = U^e(\xi^1_k, \xi^2_l, t)$ are the nodal grid-point values of the solution, and defining the test function as $\psi(\xi^1, \xi^2) = h_k(\xi^1)\, h_l(\xi^2)$. By using (84) and discrete orthogonality property of $h_k(\xi)$, we get a completely decoupled system of ODEs on Ω_e, for each grid-point (k, l) we have

$$M^e_{kl}\, \frac{d}{dt} U^e_{kl}(t) = A^e_{kl} + S^e_{kl} \tag{87}$$

$$M^e_{kl} = \int_{-1}^{1} \int_{-1}^{1} J_e\, h_k(\xi^1)\, h_l(\xi^2)\, d\xi^1 d\xi^2 = J_e(k, l)\, w_k\, w_l \tag{88}$$

$$A^e_{kl} = \sum_{i=0}^{N} J^{(1)}_e(i, l)\, F^1_{il}\, D^{(1)}_{ik}\, w_i w_l + \sum_{i=0}^{N} J^{(2)}_e(k, i)\, F^2_{ki}\, D^{(2)}_{li}\, w_k w_i \tag{89}$$

$$S^e_{kl} = J_e(k, l)\, w_k w_l\, S(U_{kl}) \tag{90}$$

where $J^{(i)}_e = J_e\, \partial\xi^i / \partial x^i$ is the metric term and $D^{(i)}_{lk}$ is the derivative matrix $h'_k(\xi^i_l)$, along x^i-direction and $i \in \{1, 2\}$. The ODEs can be written a formal matrix-vector form for Ω_e as follows: *Karniadakis and Sherwin* [2013]:

$$M^e\, \frac{d}{dt} U^e = A^e + S^e + B^e, \tag{91}$$

where M^e is the mass matrix which is diagonal, and B^e indicates the boundary terms for the element Ω_e, which is a key component linking the local and global problem (83) and enforcing C^0 continuity for solutions across element boundaries.

The global matrices associated with (83) can be obtained by summing the contributions from elemental matrices and this procedure is known as the direct stiffness summation (DSS). However the global matrices are not explicitly constructed. In practice, the DSS operation replaces interface values of two contiguous elements sharing the same physical location by the weighted sum (average) so that the boundary nodes get unique values, which maintains the continuity of the global solution across the element edges. This strategy has been adopted in CAM-SE. Note that the DSS operation does not affect interior nodal values of any element, and preserves global conservation of SE discretization for (81). The elemental discretization (91) followed by DSS operation leads the time dependent system of ODEs corresponding to (81),

$$\frac{d}{dt} U_h(t) = \mathcal{L}_h(U). \tag{92}$$

3.4 Temporal discretization

RK5

3.5 Coupling to physics

Denote the time-step for computing physics tendencies $\Delta t_{physics}$ and let $\Delta_{remap} = rsplit \times \Delta t_{dyn}$ be the vertical remapping time-step. CAM-SE uses a time-split (CHECK if it is process or time split) in which dynamics advances the model state and then the physics tendencies are based on the dynamics updated state. The question is then how to add the physics tendencies to the dynamical core. CAM-SE supports several physics-dynamics coupling methods. Let F_X be the physics tendency for prognostic variable X in level k (for notational simplicity the vertical index is dropped). The different coupling methods are detailed below and are identified with the rather arbitrary name 'ftype'. A fuller discussion with results about different coupling methods is the content of a separate paper. Some results are given in reference Jablo paper.

3.5.1 'ftype=0' configuration

In this case add $\Delta t_{remap} F_X$ to the state of X, advance the dynamics Δt_{remap} seconds based on the updated state, add $\Delta t_{remap} F_X$ to the dynamics updated state of X and advance the dynamics core, and so on. In other words, the forcing is split into $\frac{\Delta t_{physics}}{\Delta_{remap}}$ equal chunks and added throughout the dynamics.

The CAM parameterization package returns mixing ratio tendencies for tracers. We convert the mixing ratio tendencies to mass tendencies $F_x \Delta \mathcal{P}_k^{(d)}$ since the prognostic variable for tracers in the dynamical core is $\Delta p_k m_k^{(d)}$.

Generally modelers do not allow the tracer tendencies to drive the mixing ratio of tracers negative, however, this may happen using 'ftype=0'. If the tendency drives a mixing ratio negative the mixing ratio is set to zero. As a result not the entire tracer tendency is added leading to an inconsistency is how much mass the physics package wants to remove and the amount of tracer mass actually removed in the physics-dynamics coupling code in the dynamical core.

3.5.2 'ftype=1' configuration

In this configuration the entire physics forcing is added to the dynamics state $\Delta t_{physics} F_X$ which is equivalent to have the physics module update the model state. This coupling methods is used in CAM-FV [*Lin*, 2004]. Note that contrary to the 'ftype=0' configuration, this configuration always provides a closed mass budget for tracers in terms of physics tendencies being fully applied in the dynamical core.

3.5.3 'ftype=2' configuration

This configuration constitutes a hybrid approach where mass variables (tracers) used 'ftype=1' physics-dynamics coupling method and all other variables use the 'ftype=0' method.

4 2 configurations

The internal energy in CAM physics is defined as

$$I_{tot}^{(CAM)} = -\frac{1}{g} \iiint c_p^{(d)} T \left(1 + m^{(wv)}\right) \left(\frac{\partial \mathcal{P}^{(d)}}{\partial \eta^{(d)}}\right) d\eta^{(d)} \cos(\varphi) r \, d\lambda \, d\varphi. \tag{93}$$

1. Set $c_p = c_p^{(d)}$ and $\rho = \rho^{(d)} + \rho^{(wv)}$
2. Use 'correct' c_p and $\rho = \rho^{(d)} + \rho^{(wv)} + \rho^{(ci)} + \rho^{(cl)}$.

In dynamics-physics coupling we pass $\Delta p = \Delta p \left(1 + m^{(wv)}\right)$ to remain consistent with the physics definition of total energy.

5 Results

The evaluation of the SE dynamical core with CAM6 for realistic climate simulation is the subject of a separate paper. Here we ....

5.1 Idealized moist baroclinic wave with Kessler microphysics

For the validation of the new dynamical core version in a simplified setup, we use a moist variant of the dry baroclinic wave of *Ullrich et al.* [2014] with Kessler microphysics [*Kessler*, 1969]. This test case configuration was part of the Dynamical Core Model Intercomparison Project (DCMIP) 2016 test case suite [DCMIP citation]. The initialization of the atmospheric state for the moist baroclinic wave is based on analytic expressions for T_v, $\vec{v}$, p and $q^{(vw)}$ as a function of latitude and height; (φ, z). The surface geopotential is constant, $\Phi_s = 0$, and the moist surface pressure is constant $p_s = 1000hPa$. The analytical expressions for temperature, velocity components, moist pressure and specific humidity, denoted $T_v(\varphi, z)$, $\vec{v}(\varphi, z)$, $p(\varphi, z)$, and $q^{(wv)}(\varphi, z)$, respectively, are given in Appendix A: . When using a moist vertical pressure coordinate, the full level pressures p_k of the initial condition are known from the hybrid coefficients, A_k and B_k, and one can iteratively solve for z_k given moist pressure: $p_k = p(\varphi, z_k)$ [see, *Ullrich et al.*, 2014]. Once the full level heights, $z_k(\varphi)$, are known then the specific humidity, virtual temperature and velocity components can be computed by evaluating the analytical expressions at (φ, z_k). In the DCMIP 2016 test case documentation the virtual temperature is converted to temperature using $T_v = T\left(1 + \epsilon q^{(vw)}\right)$. For a dry-mass vertical coordinate model the initialization procedure is more complicated as described below.

5.1.1 Initialization of the moist baroclinic wave using a dry-mass vertical coordinate

The challenge is to extract dry pressure from the initial state defined in terms of moist pressure and preserve a balanced initial condition. For that we write the dry atmosphere hydrostatic relation (32) in terms of specific humidity, virtual temperature and moist pressure

$$\begin{aligned}
\frac{\partial \mathcal{P}^{(d)}}{\partial z} &= -\rho_d\, g, && (94)\\
&= -\frac{\rho}{1 + m^{(wv)}}\, g, && (95)\\
&= -\frac{p}{R^{(d)} T_v} \frac{1}{\left(1 + m^{(wv)}\right)}\, g, && (96)\\
&= -\frac{p}{R^{(d)} T_v} \left(1 - q^{(wv)}\right) g, && (97)
\end{aligned}$$

where we have substituted the ideal gas law and used that $\left(\frac{1}{1+m^{(wv)}}\right) = \left(1 - q^{(wv)}\right)$ for an atmosphere not containing any condensates. Hence the dry pressure as a function of latitude, φ, and height, z, is

$$\mathcal{P}^{(d)}(\varphi, z) = p_t - \int_z^{z_t} \frac{p(\varphi, z)}{R^{(d)} T_v(\varphi, z)} \left(1 - q^{(wv)}(\varphi, z)\right) g\, dz, \tag{98}$$

where z_t is the height of the model top computed by iteratively solving (A.4) with $p(\varphi, z) = p_t$ (assuming there is no moisture above the model top). To initialize the dry pressure levels a dry surface pressure is needed. It is computed by integrating (98) with lower integral bound $z = z_s = 0\,m$ and approximating the integral using 20 point Gaussian quadrature. The dry surface pressure is shown on Figure 2. The full dry pressure levels are given in terms of the hybrid coefficients $\mathcal{P}_k^{(d)}(\varphi, z_k) = A_k p_t + B_k \mathcal{P}_s^{(d)}(\varphi, z_k)$. The height, $z_k(\varphi)$, of the full dry pressure levels are computed by iteratively solving (98) with $\mathcal{P}^{(d)}(\varphi, z) = \mathcal{P}_k^{(d)}(\varphi, z_k)$. Once the heights are known the virtual temperature and velocity components can be computed by evaluating the analytical expressions at (φ, z_k) as is done for the moist vertical coordinate initialization. If we do the same for specific humidity then the moist surface pressure (which is a diagnostic when using dry-mass vertical coordinates) deviates more than 1 Pa in the tropics from the analytical value of 1000hPa (see Figure 2). As a result a spurious zonal signal in surface pressure with the same amplitude as the initial gravity waves appears in the simulations. Hence specific humidity must be initialized more carefully in order to obtain a more balanced initial condition which is discussed in the next paragraph.

As for $\mathcal{P}^{(d)}$, the weight of water vapor $\mathcal{P}^{(d)}$ per unit area can be written as

$$\mathcal{P}^{(vw)}(\varphi, z) = -\int_z^{z_t} \frac{p(\varphi, z)}{R^{(d)} T_v(\varphi, z)} q^{(wv)}(\varphi, z)\, g\, dz, \tag{99}$$

so that the moist pressure (in the absence of condensates) at half levels can be computed as the sum of dry air and water vapor pressures

$$p(\varphi, z_{k+1/2}) = \mathcal{P}^{(d)}(\varphi, z_{k+1/2}) + \mathcal{P}^{(vw)}(\varphi, z_{k+1/2}), \tag{100}$$

where $z_{k+1/2}$ is computed by the same iterative procedure as for full levels. An integrated value for water vapor in a layer can now be computed from

$$m^{(vw)}(\varphi, z_k) = \frac{p(\varphi, z_{k+1/2}) - p(\varphi, z_{k-1/2})}{\mathcal{P}^{(d)}(\varphi, z_{k+1/2}) - \mathcal{P}^{(d)}(\varphi, z_{k-1/2})} - 1. \tag{101}$$

Using this method for initializing the mixing ratio for water vapor the moist surface pressure is within 0.01 Pa of the analytical value of 10^5 Pa (see Figure 2). Once $m^{(vw)}(\varphi, z_k)$ the temperature $T(\varphi, z_k)$ can recovered from $T_v(\varphi, z_k)$ by using (14).

5.1.2 Simulation results

As part of the ‘CESM simpler models’ effort started by *Polvani et al.* [2017], the baroclinic wave setup has been implemented rigorously in the CESM in the sense that the configuration easily runs from CESM without code configurations using the ‘**FKESSLER** compset’. For instructions on how to run the moist baroclinic wave with Kessler microphysics see *Lauritzen and Goldhaber* [2017]. Since the test case configuration has been implemented in the full CESM, the dynamical core interacts with the physics module as in full climate model simulations. Hence the global energy fixer is invoked [*Williamson et al.*, 2015] and for the dynamical cores using a moist pressure vertical coordinate there is an adjustment of specific humidity to conserve water after the moist physics updates [see Section 3.1.6 in *Neale et al.*, 2010]. The intent of this implementation is to evaluate the dynamical core in simplified setup but exactly as the dynamical core is configured for comprehensive climate simulations.

Figure 3 shows the evolution of the moist baroclinic wave at day 10 using the CESM-FV [*Lin*, 2004] dynamical core, CESM1.5 version for the SE dynamical core based on a moist vertical coordinate and the new dynamical core version (CESM2.0-SE). The CESM1.5 and CESM2.0 SE dynamical cores not only differ in terms of vertical coordinates but also in terms of hyperviscosity and the formula used for the heat-capacity in the thermodynamic equation. CESM1.5-SE uses $c_p^{(d)}$ whereas CESM2.0 uses the comprehensive formula (21) that includes the heat capacity of water vapor.

Show results for wave evolution and L2 error norms

A: Analytical initial condition functions

In this section the analytical expressions for the moist baroclinic wave are given. The moist surface pressure is constant $p_s = 1000\ hPa$, meridional wind component is

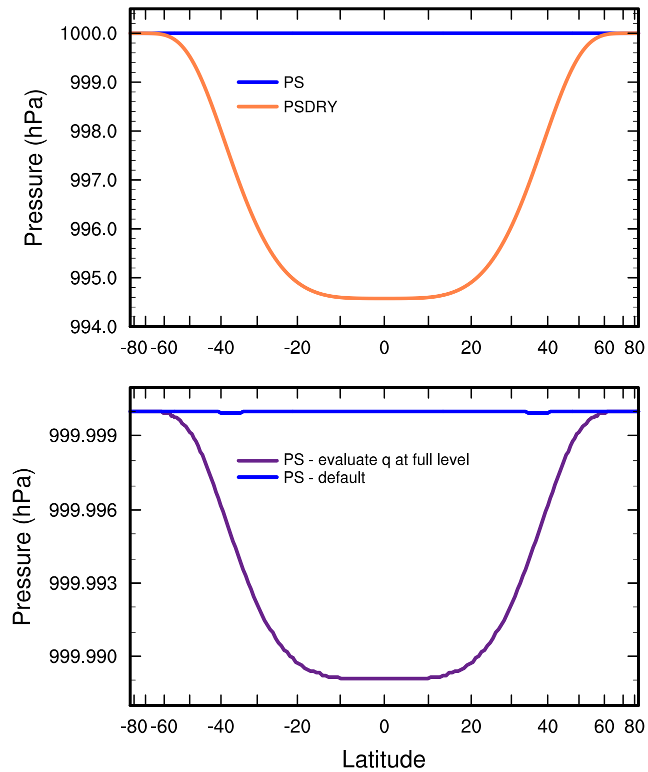

Figure 2. (Upper) Zonally averaged dry (orange) and moist (blue) surface pressure as a function of latitude for the numerically computed initial condition for the moist baroclinic wave at 1° horizontal resolution and 30 levels (CAM5 configuration). Due to increased water vapor towards the Equator the dry surface pressure decreases whereas the moist surface pressure is constant. (lower) Same as the upper plot but showing moist surface pressure where water vapor has been initialized by evaluating the analytic specific humidity formula at full levels (purple) and initializing the mixing ratio for water vapor in terms of moist and dry pressures at half levels which effectively integrates humidity over the layer (blue). Note that the upper and lower plots have different scales on the y-axis.

zero, $v(\varphi, z) = 0\ m/s$, and the surface geopotential is zero, $\Phi_s(\varphi, z) = 0\ m^2/s^2$. The reference virtual temperature is given by

$$T_v(\varphi, z) = \left\{ \mathcal{F}_1(z) - \mathcal{F}_2(z) \left[(\cos\varphi)^{\mathcal{K}} - \frac{\mathcal{K}}{\mathcal{K}+2} (\cos\varphi)^{\mathcal{K}+2} \right] \right\}^{-1}, \tag{A.1}$$

where

$$\mathcal{F}_1(z) = \frac{1}{T_0} \exp\left(\frac{\Gamma z}{T_0}\right) + \left(\frac{T_0 - T_P}{T_0 T_P}\right) \left[1 - 2\left(\frac{zg}{bR^{(d)}T_0}\right)^2\right] \exp\left[-\left(\frac{zg}{bR^{(d)}T_0}\right)^2\right] \tag{A.2}$$

$$\mathcal{F}_2(z) = \frac{(\mathcal{K}+2)}{2} \left(\frac{T_E - T_P}{T_E T_P}\right) \left[1 - 2\left(\frac{zg}{bR^{(d)}T_0}\right)^2\right] \exp\left[-\left(\frac{zg}{bR^{(d)}T_0}\right)^2\right], \tag{A.3}$$

with $T_0 = \frac{1}{2}(T_E + T_P)$. Parameter $T_E = 310\ \mathcal{K}$ is the temperature at the Equatorial surface, $T_P = 240\ \mathcal{K}$ is the polar surface temperature, $\mathcal{K} = 3$ is the jet width parameter, $b = 2$ is the jet half-width parameter, and $\Gamma = 0.005\ K/m$ is the lapse rate.

To maintain hydrostatic balance, the pressure is given by:

$$p(\varphi, z) = p_0 \exp\left[-\frac{g}{R^{(d)}} \left(\mathcal{F}_3(z) - \mathcal{F}_4(z) \mathcal{I}_T(\varphi)\right)\right] \tag{A.4}$$

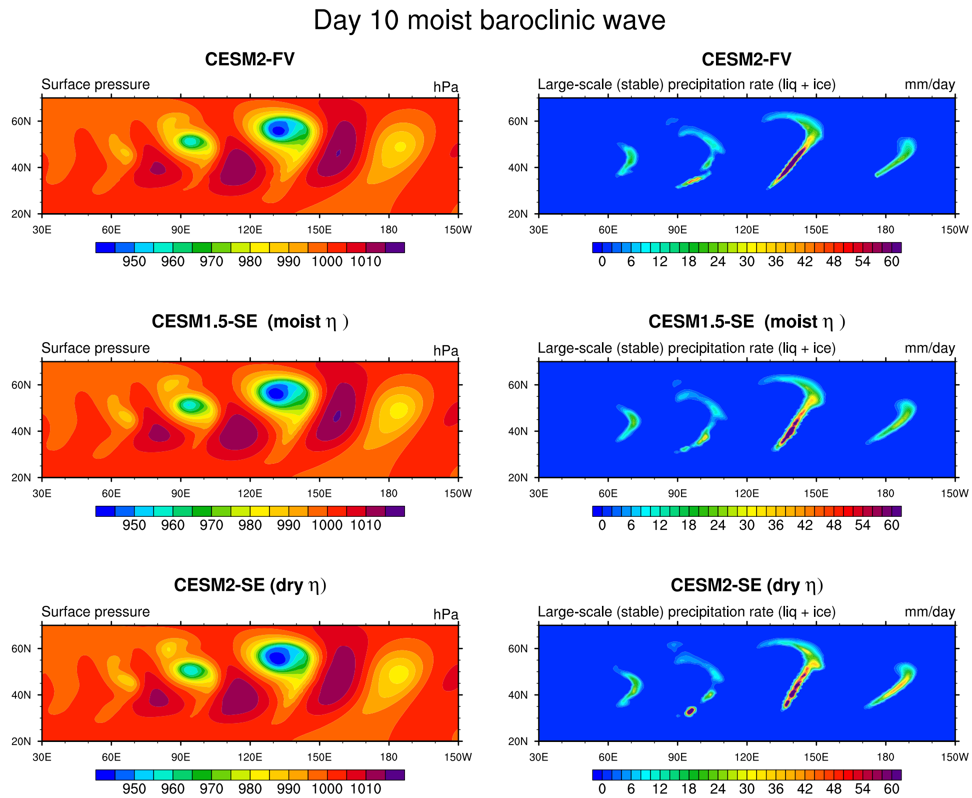

Figure 3. Left column shows moist surface pressure at day 10 for the moist baroclinic wave test case for (row 1) the finite-volume dynamical core, (row 2) CESM1.5 version of the SE dynamical core based on a moist pressure vertical coordinate and (row 3) the dry-mass vertical coordinate version of SE presented in this paper. Rights column is the same as the left but for large-scale precipitation rate.

where

$$\mathcal{F}_3(z) = \frac{1}{\Gamma}\left[\exp\left(\frac{\Gamma z}{T_0}\right) - 1\right] + z\left(\frac{T_0 - T_P}{T_0 T_P}\right)\exp\left[-\left(\frac{zg}{bR^{(d)}T_0}\right)^2\right] \tag{A.5}$$

$$\mathcal{F}_4(z) = \frac{(\mathcal{K}+2)}{2}\left(\frac{T_E - T_P}{T_E T_P}\right) z \exp\left[-\left(\frac{zg}{bR^{(d)}T_0}\right)^2\right]. \tag{A.6}$$

To define the zonal velocity component define the great circle distance between (λ, φ) and (λ_p, φ_p):

$$r(\lambda, \varphi; \lambda_p, \varphi_p) = a \arccos\left(\sin\varphi \sin\varphi_p + \cos\varphi \cos\varphi_p \cos(\lambda - \lambda_p)\right). \tag{A.7}$$

The zonal velocity component is

$$u(\varphi, z) = -\Omega a \cos(\varphi) + \sqrt{(\Omega a \cos(\varphi))^2 + a\cos(\varphi) U(\varphi, z)} + u'(\lambda, \varphi, z), \tag{A.8}$$

where the zonally symmetric part of the velocity field is given by

$$U(\varphi, z) = \frac{g\mathcal{K}}{a}\mathcal{F}_4(z)\left[(\cos\varphi)^{\mathcal{K}-1} - (\cos\varphi)^{\mathcal{K}+1}\right] T_v(\varphi, z), \tag{A.9}$$

$a = 6371.22\ m$ is the mean radius of Earth and angular velocity is $\Omega = \frac{2\pi}{86164}\ \frac{1}{s}$ (denominator is length of day is seconds), and $u'(\lambda, \varphi, z)$ is the exponential bell-shaped perturbation to the zonally balanced velocity field

$$u'(\lambda, \varphi, z) = \begin{cases} U_p Z(z) \exp\left[-\left(\frac{r(\lambda,\varphi;\lambda_p,\varphi_p)}{r_p}\right)^2\right], & \text{if } r(\lambda, \varphi; \lambda_p, \varphi_p) < r_p, \\ 0, & \text{otherwise,} \end{cases} \tag{A.10}$$

where perturbation velocity is $U_p = 1\ m/s$, longitude/latitude of the zonal wind perturbation centerpoint is (λ_p, φ_p)=$(\pi/9, 2\pi/9)$=(20°E,40°N), and

$$Z(z) = \begin{cases} 1 - 3\left(\frac{z}{z_p}\right)^2 + 2\left(\frac{z}{z_p}\right)^3, & \text{if } z \leq z_p, \\ 0, & \text{otherwise,} \end{cases} \tag{A.11}$$

where $z_p = 15000\ m$ is the maximum height of the zonal wind perturbation. The specific humidity (moist mixing ratio for water vapor) is specified in terms of moist pressure (as the vertical variable)

$$q^{(vw)}(\lambda, \varphi, p) \quad = \quad \begin{cases} q_0 \exp\left[-\left(\frac{\varphi}{\varphi_w}\right)^4\right] \exp\left[-\left(\frac{p-p_0}{p_w}\right)^2\right], & \text{if } p > p_0/10, \\ q_t, & \text{otherwise.} \end{cases} \tag{A.12}$$

where $p_w = 340\ hPa$ is a pressure width parameter, $q_0 = 0.018\ kg/kg$ is maximum specific humidity, $q_t = 1.0 \times 10^{-12}\ kg/kg$ is specific humidity above artificial tropopause, $\varphi_w = 2\pi/9$ is the specific humidity latitudinal width parameter. In addition to water vapor the Kessler microphysics water species are cloud liquid, $m^{(cl)}$, and rain water, $m^{(rw)}$. Both are initialized to zero kg/kg.

Acknowledgments
= enter acknowledgments here =

References

Colella, P., and P. R. Woodward (1984), The piecewise parabolic method (PPM) for gas-dynamical simulations, *J. Comput. Phys.*, *54*, 174–201.

Dennis, J. M., J. Edwards, K. J. Evans, O. Guba, P. H. Lauritzen, A. A. Mirin, A. St-Cyr, M. A. Taylor, and P. H. Worley (2012), CAM-SE: A scalable spectral element dynamical core for the Community Atmosphere Model, *Int. J. High. Perform. C.*, *26*(1), 74–89, doi:10.1177/1094342011428142.

Karniadakis, G., and S. Sherwin (2013), *Spectral/hp element methods for computational fluid dynamics*, Oxford University Press.

Kasahara, A. (1974), Various vertical coordinate systems used for numerical weather prediction, *Mon. Wea. Rev.*, *102*(7), 509–522.

Kessler, E. (1969), On the distribution and continuity of water substance in atmospheric circulations, *Meteorol. Monogr.*, *10*(32), 88.

Lauritzen, P., and J. Thuburn (2012), Evaluating advection/transport schemes using interrelated tracers, scatter plots and numerical mixing diagnostics, *Quart. J. Roy. Met. Soc.*, *138*(665), 906–918, doi:10.1002/qj.986.

Lauritzen, P. H., and S. Goldhaber (2017), *CESM simpler models: Moist baroclinic wave with Kessler microphysics*, `http://www.cesm.ucar.edu/models/simpler-models-indev/fkessler/index.html`.

Lin, S.-J. (2004), A 'vertically Lagrangian' finite-volume dynamical core for global models, *Mon. Wea. Rev.*, *132*, 2293–2307.

Nair, R., H.-W. Choi, and H. Tufo (2009), Computational aspects of a scalable high-order discontinuous galerkin atmospheric dynamical core, *Computers & Fluids*, *38*(2), 309 – 319, doi:http://dx.doi.org/10.1016/j.compfluid.2008.04.006.

Nair, R. D., S. J. Thomas, and R. D. Loft (2005), A discontinuous Galerkin global shallow water model, *Mon.Wea.Rev.*, *133*, 876–888.

Neale, R. B., C.-C. Chen, A. Gettelman, P. H. Lauritzen, S. Park, D. L. Williamson, A. J. Conley, R. Garcia, D. Kinnison, J.-F. Lamarque, D. Marsh, M. Mills, A. K. Smith, S. Tilmes, F. Vitt, P. Cameron-Smith, W. D. Collins, M. J. Iacono, R. C. Easter, S. J. Ghan, X. Liu, P. J. Rasch, and M. A. Taylor (2010), Description of the NCAR Community Atmosphere Model (CAM 5.0), *NCAR Technical Note*, National Center of Atmospheric Research.

Polvani, L., A. Clement, B. Medeiros, J. Benedict, and I. Simpson (2017), Opening the door to simpler climate models in the commnity earth system model project, *EOS*, submitted.

Sadourny, R. (1972), Conservative finite-difference approximations of the primitive equations on quasi-uniform spherical grids, *Mon. Wea. Rev.*, *100*, 136–144.

Simmons, A. J., and D. M. Burridge (1981), An energy and angular-momentum conserving vertical finite-difference scheme and hybrid vertical coordinates, *Mon. Wea. Rev.*, *109*(4), 758–766.

Staniforth, A., A. White, N. Wood, J. Thuburn, M. Zerroukat, E. Cordero, T. Davies, and . M. Diamantakis (2006), Joy of u.m. 6.3 - model formulation, *UK Met Office Technical Note*, *15*.

Starr, V. P. (1945), A quasi-Lagrangian system of hydrodynamical equations., *J. Atmos. Sci.*, *2*, 227–237.

Taylor, M., J. Edwards, and A. St-Cyr (2008), Petascale atmospheric models for the community climate system model: new developments and evaluation of scalable dynamical cores, *J. Phys.: Conf. Ser.*, *125*, doi:10.1088/1742-6596/125/1/012023.

Taylor, M. A. (2011), Conservation of mass and energy for the moist atmospheric primitive equations on unstructured grids, in: P.H. Lauritzen, R.D. Nair, C. Jablonowski, M. Taylor (Eds.), Numerical techniques for global atmospheric models, *Lecture Notes in Computational Science and Engineering, Springer, 2010, in press.*, *80*, 357–380, doi: 10.1007/978-3-642-11640-7_12.

Thomas, S., and R. Loft (2000), Parallel semi-implicit spectral element methods for atmospheric general circulation models, *J. Sci. Comput.*, *15*, 499–518.

Ullrich, P. A., T. Melvin, C. Jablonowski, and A. Staniforth (2014), A proposed baroclinic wave test case for deep and shallow-atmosphere dynamical cores, *Quart. J. Royal Meteor. Soc.*, *140*(682), 1590–1602.

Williamson, D. L., J. G. Olson, C. Hannay, T. Toniazzo, M. Taylor, and V. Yudin (2015), Energy considerations in the community atmosphere model (cam), *J. Adv. Model. Earth Syst.*, *7*(3), 1178–1188, doi:10.1002/2015MS000448.